FOLIA HISTOCHEMICA ET CYTOBIOLOGICA
Vol. 56, No. 4, 2018
pp. 185–194

ORIGINAL PAPER

VIA MEDICA

Semispecific TPPII inhibitor Ala-Ala-Phe-chloromethylketone (AAF-cmk) displays cytotoxic activity by induction of apoptosis, autophagy and protein aggregation in U937 cells

Lukasz P. Bialy[1, *], Jean Fayet[2], Grzegorz M. Wilczynski[3], Izabela Mlynarczuk-Bialy[1, *]

[1]Department of Histology and Embryology, Center for Biostructure Research, Medical University of Warsaw, Warsaw, Poland

[2]Department of Ophthalmology, First Medical Faculty, Medical University of Warsaw, Warsaw, Poland

[3]Laboratory of Molecular and Systemic Neuromorphology, Department of Neurophysiology, Nencki Institute of Experimental Biology, PAN, Warsaw, Poland

[*]Both authors contributed equally to this work

Abstract

Introduction. The main component of extralysosomal proteolysis is the ubiquitin-proteasome system (UPS), which is supplemented by tripeptidyl peptidase II (TPPII). That system is a target for anticancer strategies by using proteasome inhibitors. Data from several studies on leukemic cells share evidence for the beneficial and potential role of TPPII in cell survivability. Therefore, the aim of this work was to analyze the effect of AAF-cmk, a membrane permeable semi-specific TPPII inhibitor, on human monocytic leukemic cells U937 for translational research.

Material and methods. We studied the viability of U937 cells incubated with AAF-cmk using tetrazolium salt reduction assay (MTT) and apoptosis induction by assessing caspase activation by Western blotting and Annexin V binding assays. Transmission electron microscopy (TEM), a gold standard for apoptosis and autophagy detection, was used to assess the ultrastructure of U937 cells.

Results. Incubation of cells with AAF-cmk reduced their viability and induced apoptosis by intrinsic pathway. In groups treated with AAF-cmk, activation of caspases 9 and 3 was observed and caspase inhibition by zVDA restored cell viability. TEM revealed the presence of ultrastructural features of apoptosis and authophagy. Moreover, we identified two types of protein aggregates. The first one was found in close proximity to the endoplasmic reticulum (ER) and corresponds to Aggresome-Like Structure (ALIS); however, the second novel type of aggregate was not related to ER elements, but rather to free cytosolic ribosomes. This type did not correspond to the aggresome neither in localization nor the structure, thus we referred these aggregates as ALiSNER (Aggresome-Like Structure Not Associated With the ER).

Conclusions. Our results provide novel and important findings about the role of TPPII in protein homeostasis and cell survival. Since semispecific TPPII inhibitor AAF-cmk displays cytotoxic activity against leukemic U937 cells *in vitro* it can be considered as a potential anticancer agent. *(Folia Histochemica et Cytobiologica 2018, Vol. 56, No. 4, 185–194)*

Key words: U937 cells; AAF-cmk; TPPII; apoptosis; autophagy; proteasome; aggresome; TEM; ALiSNER

Correspondence address: L.P. Bialy
Department of Histology and Embryology,
Center for Biostructure Research,
Medical University of Warsaw, Poland
Chałubinskiego 5, 02–004 Warsaw, Poland
e-mail: lbialy@esculap.pl

Introduction

Tripeptidyl peptidase II (TPPII) is the largest known protease complex in eukaryotic cells (6MDa) [1]. TPPII involvement in several cellular processes has been previously described; however, presently its function still remains enigmatic [2]. This giant peptidase acts primarily downstream of the ubiquitin-proteasome system (UPS), by degrading and trimming oligopeptides generated by the proteasome [3–6].

In normal conditions, the function of TPPII can be replaced by other proteases, as has been demonstrated in studies in TPPII-deficient mice [7]. However, during periods of stress in addition to states affecting the function of UPS, TPPII has been shown to support and substitute the UPS-dependent cytoplasmic proteolysis maintaining homeostasis in the cell [8].

Available data indicate that TPPII plays a role in the proliferation and survival of malignant lymphoid cells. For example, up-regulation of TPPII was reported in EL4 lymphoma cells adapted to grow in the presence of proteasome inhibitors [5, 9]. Conversely, transfection resulting in the overexpression of TPPII, generated increased resistance of lymphoma cells against proteasome inhibitors as compared to the control non-transfected cells [10]. Accelerated cell growth and mitotic infidelity with centrosome duplication errors were observed in cells overexpressing TPPII. Inhibition or siRNA silencing of TPPII in these cells resulted in mitotic aberrations and diminished cell division rate [11, 12]. In addition, overexpression of TPPII protected cells against activity of mitotic inhibitors [13].

The overexpression of some oncogenes, for example c-myc, resulted in up-regulation of TPPII [14]. Furthermore, it was shown that treatment of Burkitt lymphoma cells with upregulated TPPII expression with AAF-cmk, a membrane permeable semi-specific TPPII inhibitor, reduced cell proliferation and induced apoptosis [14]. The similar effect was observed in c-myc overexpressing Burkitt lymphoma cells for more specific but low membrane permeable TPPII inhibitor — butabindide [15].

Cancer cells can adopt proteolytic machinery to the stressful conditions inside a tumor including increased deubiquitination or decreased proteasome activity that results in resistance to proteasome inhibitors and increased activity of TPPII [14, 16]. For example, stress related with nutritional starvation, resulted in TPPII upregulation in lymphoma cells both *in vitro* and *in vivo* [16]. These observations have given rise to the hypothesis that TPPII contributes to antiapoptotic phenotype of some cancer cells [11].

Moreover, exposure to DNA-damaging anticancer drugs, led to TPPII translocation from the cytoplasm to the cell nucleus in the MAP kinase-dependent pathway [17]. The inhibition of TPPII by AAF-cmk can synergistically potentiate cell death induced by pro-apoptotic cytokines, as it was shown for TRAIL and TNFα in human leukemic U937 cells [18].

AAF-cmk is an irreversible cell membrane permeable inhibitor of TPPII. In cellular models (human renal carcinoma BB64-RCC and human embryonic kidney HEK293 or leukemic EL4) AAF-cmk effectively inhibits the TPPII activity when added to the cell culture at concentration starting from 5 μM [5, 19, 20]. However, in concentrations higher than 50 μM AAF-cmk also inhibits bleomycin hydrolase and puromycin-sensitive aminopeptidase [21] and may interfere with the chymotrypsin-like activity of the proteasome [6]. Therefore, for our study we used AAF-cmk at concentrations lower than 50 μM, which is declared as TPPII specific.

The aim of the study was to examine the effect of AAF-cmk on proliferation, apoptosis, and ultrastructure of human leukemic U937 cells to gain insight into the intracellular alterations induced by this cell membrane-permeable TPTII inhibitor.

Material and methods

Reagents. Ala-Ala-Phe-chloromethylketone, AAF-cmk and z-VAD-fmk (all purchased from Sigma, St. Louis, MO, USA) were dissolved in dimethylsulfoxide (DMSO) and stored as a 10 mM stock solutions at –20°C. Recombinant human TNF (rhTNF produced in *E. coli* was kindly provided by Dr. W. Stec (Department of Bioorganic Chemistry, Center of Molecular and Macromolecular Studies, Lodz, Poland). The specific activity of the rhTNFα was $4.3 \pm 1.1 \times \times 10^7$ U/mg protein.

Cell culture. U937 cells (ATCC) were cultured in standard conditions as described in [18]. Shortly, cells were cultured in RPMI-1640 medium with stable glutamine (Biochrom, Berlin, Germany) supplemented with 10% heat-inactivated fetal calf serum (FCS) (Biochrom), 1% Antibiotic–Antimycotic (Thermo Fisher/LifeTechnologies, Waltham, MA, USA) in 25 cm^2 tissue flasks (Greiner, Berlin, Germany) and kept at 37°C in a 5% CO_2 humidified atmosphere and passaged every 2–3 days.

Cytotoxicity assay. The cytostatic/cytotoxic effects of AAF--cmk on U937 cells *in vitro* was assayed by a standard MTT test as previously described [22]. Cells (5×10^3) were dispensed into 96-well microtiter plates (Becton Dickinson, Franklin, NJ, USA) and incubated with AAF-cmk and/or with pan-caspase inhibitor zVAD-fmk 4 h before addition

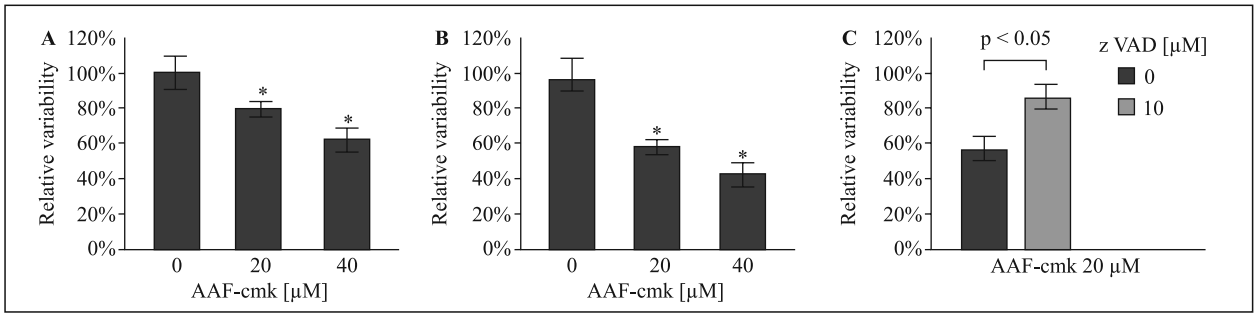

Figure 1. Viability of U937 cells incubated with AAF-cmk. **A.** U937cells were incubated with AAF-cmk or DMSO solvent at given concentrations for 24 h. **B.** U937 cells were incubated with AAF-cmk or DMSO solvent at given concentrations for 48 h. **C.** U937 cells were pre-incubated with pan-caspase inhibitor zVAD-fmk for 4 h, and then with AAF-cmk for next 48 h. Cell viability was assessed by MTT assay as described in Methods. Results are expressed in relation to viability of control cells incubated with of DMSO solvent. Bars represent means and SD. *significantly different from control, $p < 0.05$ (Student t-test).

of AAF-cmk for 48 h in a final volume of 200 μL/well. Appropriate volumes of culture medium, supplemented with DMSO (< 0.1%) were added as controls. Plates were read on an FLUOstar Omega Microplate Reader (BMG LABTECH, Ortenberg, Germany) using a 550 nm filter. Cytostatic/cytotoxic effect was expressed as relative viability of control U937 cells [22].

Annexin V binding assay. Phosphatidylserine externalization of apoptotic cells was visualized by staining with annexin V-FITC Fluorescence Microscopy Kit according to the manufacturer's instructions (Becton Dickinson). The number of Annexin V-FITC positive cells was calculated under JuliStage epifluorescent microscope (NanoEnTek, Seoul, Korea).

Western blot analysis and antibodies. Cell lysates were assayed by a standard SDS-PAGE, subjected to semi-dry transfer onto nitrocellulose membrane and probed with appropriate primary and secondary antibody (all from Santa Cruz Biotechnology, Santa Cruz, CA, USA). The signal was visualized by the chemiluminescence method described by Mlynarczuk-Bialy *et al.* [23].

Transmission electron microscopy. For electron microscopy cells were double washed in phosphate-buffered saline (PBS) and immediately fixed in 2.5% glutaraldehyde EM grade (Merck, Darmstadt, Germany) and 2% paraformaldehyde (Sigma, St. Louis, MO, USA) in 0.1 M cacodylate buffer (pH 7.4) for 1.5 h, postfixed in 1% OsO_4 in 0.1 M cacodylate buffer (pH 7.4) for 1 h, dehydrated in graded alcohol and embedded in Spurr resin (Sigma). Ultrathin sections were placed onto copper grids and contrasted with uranyl acetate and lead citrate (Merck). The sections were observed at 5500–6000× primary magnification with a JEOL JEM 100 S electron microscope (Jeol, Tokyo, Japan) at 80 kV.

Statistical analysis. Data was presented as means and standard deviation (SD). Differences between groups were analyzed for significance by Student's *t*-test using Microsoft Excel (Microsoft, Redmond, WA, USA). A series of independent experiments were performed and the results presented in the paper are representative.

Results

AAF-cmk decreases viability of U937 leukemic cells

An MTT assay was used to assess the influence of AAF-cmk on cell viability. The results are displayed as percentage of control cells that were incubated with corresponding volume of AAF-cmk solvent.

AAF-cmk displayed cytotoxic/cytostatic effect on leukemic U937 cells in a time- and dose-dependent manner. After 24 h of incubation with AAF-cmk, cell viability was moderately reduced for both (20 μM and 40 μM) concentrations. The cell viability was reduced to 61.2% ± 5.16 (mean and standard deviation) for 40 μM AAF-cmk, whereas 20 μM AAF-cmk reduced it to 79.4% ± 2.34 (Fig. 1A). After 48 h of incubation with the inhibitor, cell viability was reduced to 5 9.2% ± 2.65 and 41.5% ± 2.45 for 20 μM and 40 μM AAF-cmk, respectively (Fig. 1B). The calculated IC50% for 48 h of AAF-cmk was 30 μM.

Caspase inhibition restores the viability of AAF-cmk-treated cells

To further characterize the nature of AAF-cmk inhibitory effect on cell viability, we investigated the effect of pan-caspase inhibitor z-VAD-fmk on the viability of cells incubated with AAF-cmk.

As shown in Figure 1C, the inhibition of caspases partially eliminated negative action of AAF-cmk on cell viability. In AAF-cmk-treated cells (20 μM, 48 h), viability was reduced to 59.2% ± 5.18 and in the group

pre-incubated with z-VAD-fmk and subsequently incubated with both agents for 48 h it reached 84.8% ± ± 4.43. Thus, the addition of z-VAD-fmk recovered the viability by ca. 25% in comparison to AAF-cmk alone.

AAF-cmk triggered activation of apoptotic caspases

In order to better characterize caspase dependence of AAF-cmk inhibitory action on cell viability, we investigated the activation of apoptotic caspases in AAF-cmk-treated cells by Western blotting. TNF was used as a positive control of apoptosis induction.

As shown in Figure 2A, after incubation with cells for 24 h, AAF-cmk (20 μM and 40 μM) led to the activation of caspase-9 (lines 2 and 3 left), which is responsible for initiating the intrinsic apoptotic pathway. We did not observe significant signal in the control group (line 1 left), with only slight signal in TNF-treated cells (line 4 left). Hence, the signal for active caspase-9 was significantly weaker after prolonged incubation of cells with AAF-cmk (20 μM and 40 μM) for 48 h (lines 2 and 3 right).

Following AAF-cmk treatment for 48 h, a strong activation of the executor caspase-3 was observed in U937 cells incubated with 40 μM AAF-cmk (line 3 right). Additionally, the caspase substrate PARP demonstrated strong cleavage in these cells. Lower signal for active caspase-3 was noted in the group treated with 20 μM AAF-cmk (line 4 right) and after 24 h of AAF-cmk treatment for both inhibitor concentrations (lines 2 and 3 left). Furthermore, signal for cleaved form of PARP was lower in the same groups. In the control cells, there was no active caspase-3 signal present, and the signal for cleaved PARP form was low (lines 1 left and right). The positive apoptosis inducer TNF caused strong caspase-3 activation and PARP cleavage in both incubation periods (lines 4 left and right).

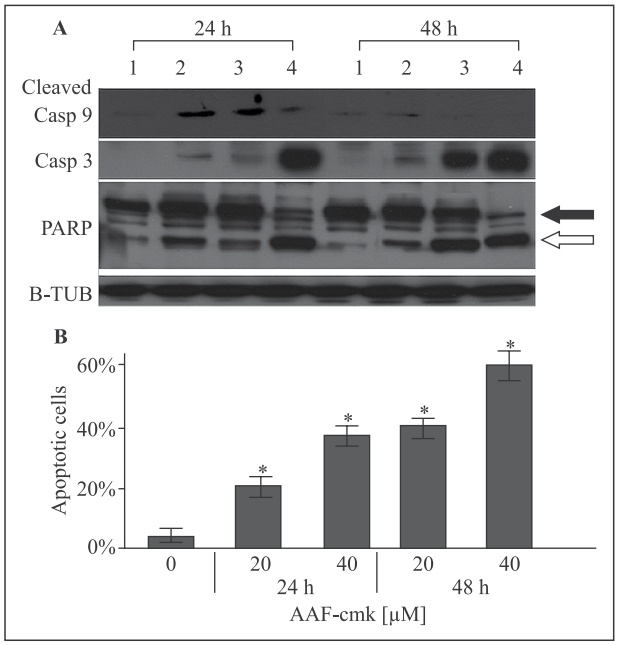

Figure 2. Apoptosis induction in U937 by AAF-cmk. **A.** Caspases activation and PARP cleavage by AAF-cmk in U937 leukemic cells. U937 cells were incubated for 24 h or 48 h with: line 1 — DMSO (control), line 2 — AAF-cmk 20 μM, line 3 — AAF-cmk 40 μM, line 4 — TNF (0.01 ng/ml — positive control). Cleaved caspase 9 and 3, PARP was analyzed by Western-blotting with appropriate antibodies. β-tubulin displayed as a loading control. **B.** Phosphatidylserine externalization induced by AAF-cmk in U937 leukemic cells. U937 cells were incubated with AAF-cmk or DMSO solvent at given concentrations for 24 h and 48 h. Phosphatidylserine externalization was detected by AnnexinV-FITC staining. Bars represent means and SD. *significantly different from control, $p < 0.05$ (Student t-test).

AAF-cmk induces externalization of phosphatidylserine in U937 cells

An Annexin V-FITC assay was performed to quantify effects of AAF-cmk on apoptosis.

As shown in Figure 2B (dark columns), we observed a dose and time-dependent increase in cells positive for Annexin V-FITC. In control groups, we observed a minimal ratio of Annexin V-FITC positive cells.

The maximal amount of Annexin V binding cells was detected after 48 h in cells incubated with 40 μM AAF-cmk. In this group 61.2% ± 8.56 of cells were positive for Annexin V-FITC whereas in the cells treated with 20 μM AAF-cmk for 48 h — 41.5% ± ± 6.25. Hence, after incubation for 24 h the percentage of annexin positive cells was 20.5% ± 6.25 for 20 μM and 37.8% ± 4.25 for 40 μM AAF-cmk (Fig. 2B).

AAF-cmk evokes ultrastructural hallmarks of apoptosis and autophagy with ALiSNER formation

Following 24 h of incubation, the lower AAF-cmk concentration (20 μM) did not demonstrate evident ultrastructural features of apoptosis (Fig. 3A).

Cells incubated with higher AAF-cmk concentration (40 μM) after the same time, early apoptotic signs were observed including: (1) irregular condensation of chromatin under the nuclear envelope, (2) electron-translucent crescent shaped spaces (CSS) in perinuclear area (Fig. 3B) corresponding to ultrastructural stage I of apoptosis. The higher AAF-cmk concentration (40 μM) at the 24h time point featured numerous electron-translucent vesicles and autophagic structures of ER-origin (Fig. 3B, G).

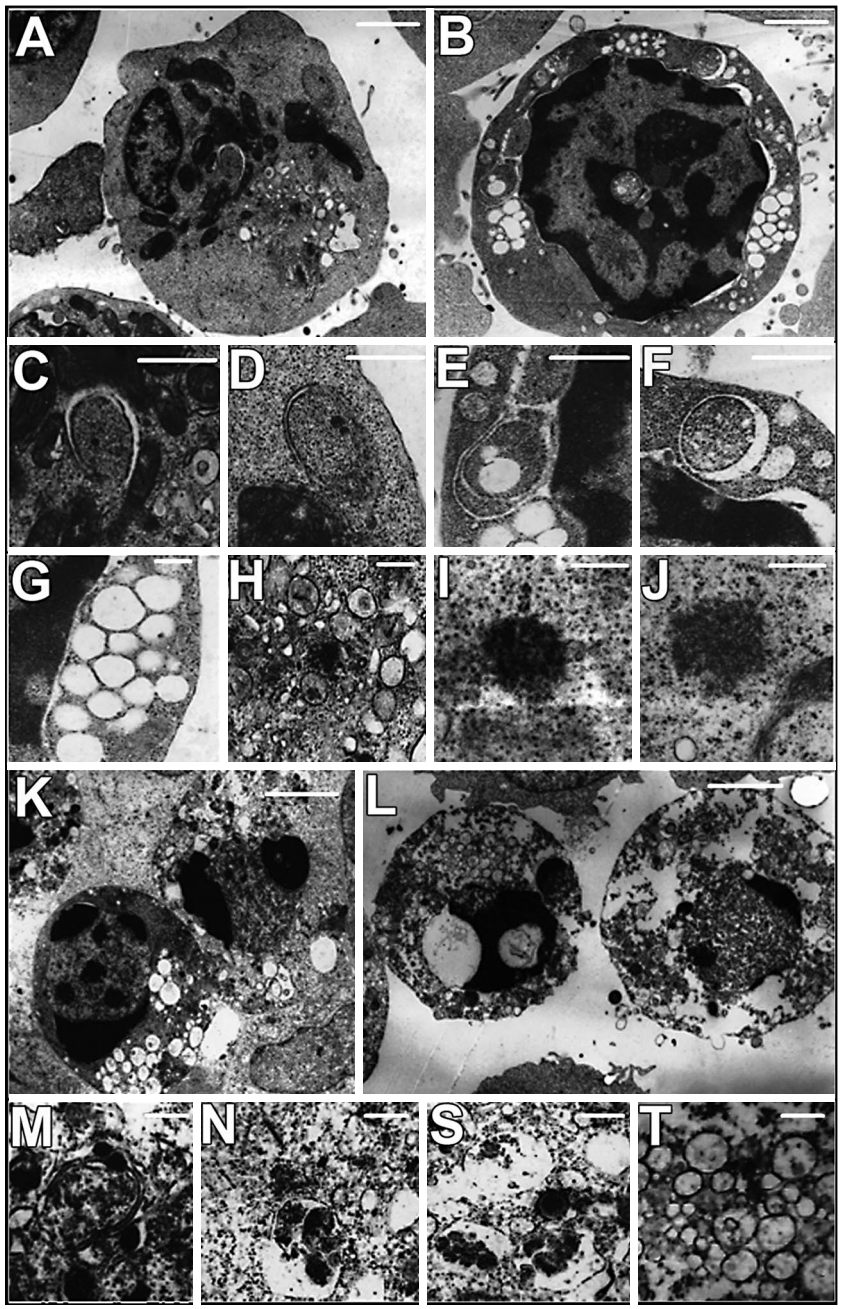

Figure 3. Ultrastructure of U937 cell incubated with AAF-cmk for 24 or 48 hours. **A–J:** U937 cells were treated with AAF-cmk for 24 h. **A.** AAF-cmk 20 μM. **B.** AAF-cmk 40 μM. **C–E.** Autophagosome formation (phagophore): C, D — AAF-cmk 20 Mm; E — AAF-cmk 40 μM. **F.** Early double-membrane autophagosome (AAF-cmk 40 μM). **G.** Vacuolization of endoplasmic reticulum (ER) at 40 μM AAF-cmk. **H.** Aggresome-like structure (ALIS) within the ER-rich cytoplasm at AAF-cmk. **I–J.** ALiSNER within the cytoplasm surrounded by ribosomes at 20 μM AAF-cmk, and 40 μM AAF-cmk (J). **K–T:** U937 cells were treated with AAF-cmk for 48 h. **K.** The representative cells incubated with AAF-cmk 20 μM. **L.** The representative cells incubated with AAF-cmk 40 μM. **M-S.** Secondary autophagic structures (AAF-cmk 20 μM). **T.** Secondary regressive changes in cytoplasm (AAF-cmk 40 μM). Scale bars: A, B — 2.50 μm; C, F — 1 μm; G — 100 nm; H — 500 nm; I, J — 200 nm; K, L — 5 μm; M-T — 500 nm.

As shown in Figs 3C and 3D, autophagy was initiated by phagophore formation *via* engulfment of cytoplasm by isolation membranes (at the lower inhibitor concentration). Phagophores were observed as cup-shaped structures of ER origin. Higher inhibitor concentration resulted in presence of more advanced autophagic structures (Fig. 3E, F). Autophagosome formation was observed as a double membrane struc-

ture with an electron-translucent space between them (Fig. 3F). Apart from electron-translucent vacuoles, a number of vesicles containing digested material representing lysosomes were observed (Fig. 3G). Among these structures of ER-rich cytoplasm, electron-dense aggregates of proteins were noted (Fig. 3H). The second type of aggregate was found in close proximity to free cytosolic ribosomes (Fig. 3I, J).

After 48 h of the incubation of cells with the studied inhibitor, late apoptotic and late autophagic characteristics were observed. Chromatin underwent further condensation while the nuclei were occasionally fragmented (Fig. 3K, L). The cytoplasm underwent secondary regressive changes leading to cytoplasm disintegration.

As visualized in Figure 3K in U937 cells incubated for 24 h with lower AAF-cmk concentration (20 μM), the chromatin was condensed as either non-protruding crescents (left cell), or large formed clumps which pressed against the nuclear envelope forming buds (right cell), corresponding to the ultrastructural stage II of apoptosis.

The incubation with higher concentration of AAF-cmk (40 μM) resulted in nuclear fragmentation by pinching off nuclear fragments (Fig. 3L left cell) or nuclear disintegration (Fig. 3L right cell). The ultrastructural changes in this group represented stage III of apoptosis accompanied by secondary regressive necrotic changes.

The late autophagic changes, included presence of autophagolysosomes with electron-dense digested material (Fig. 3M, N, S). Numerous vesicles of lysosomal origin were also visualized within the cytoplasm (Fig. 3T).

Discussion

Extralysosomal proteolysis is involved in the regulation of many key cellular processes through the degradation of crucial regulatory proteins that are involved in mediating cell proliferation and cell death [24]. The main component of this protein breakdown pathway is the proteasome which is supplemented by action of TPPII.

Two TPPII inhibitors are available commercially: AAF-cmk and butabindide. AAF-cmk inhibitor is potent irreversible, and membrane permeable [5, 20, 25]. It slightly but not significantly interferes with the chymotrypsin-like activity of the proteasome [6]. However, in concentrations higher than 50 μM it inhibits also bleomycin hydrolase and puromycin-sensitive aminopeptidase and other serine and cysteine proteases [21]. For this reason we have used AAF-cmk in concentration lower than 50 μM. However, the interpretation of any biological effects of AAF-cmk in terms of TPPII inhibition must be done with caution.

Butabindide is a TPPII specific reversible and competitive inhibitor but has low membrane permeability [26–28]. Moreover it is instable in aqueous solutions and even small amounts of fetal calf serum in culture media prevent the inhibitory effect of butabindide *in vitro,* thus, its action can be observed only in serum-free systems [26, 29]. Therefore, all negative results obtained using butabindide as the inhibitor [30] must be treated very warily so that AAF-cmk has better transitional potential for any clinical application. Recently, a novel selective, irreversible membrane permeable inhibitor of TPPII, B6, was reported but up to now it is not commercially available [31]. Furthermore, siRNA-based inhibitory strategies are also no perfect for TPPII silencing because they allow to obtain a downregulation of TPPII expression only up to sixty percent [29]. Taken into consideration all information given above AAF-cmk has the best translational potential among the available TPPII inhibitory strategies and was used by us in this study in the concentrations declared as TPPII specific.

Targeting extralysosomal proteolysis by proteasome inhibitors is a well established anticancer strategy, especially in hematological malignancies. The hematological cell line U937, which is of human monocytic leukemia origin, was demonstrated to be very sensitive to proteasome inhibition [32]. In this study, we showed that the incubation of U937 cells with AAF-cmk results in cell death by inducing apoptosis and autophagy.

Apoptosis induction is a preferable anti-tumor strategy in tumor therapy, and this process of cell death is induced by several anticancer agents [33]. Biochemically, apoptosis is initiated and executed by the action of caspases that lead to nuclease activation and thereby internucleosomal DNA cleavage. Apoptosis can be designated into two pathways: intrinsic, through the recruitment of caspase 9, and extrinsic, which is activated by various ligands including TNF. Both pathways lead to the activation of caspase 3 as a common pathway. The plasma membrane of the apoptotic cell is intact but undergoes changes in phospholipid distribution. Phosphatidylserine is externalized from the inner to outer plasma membrane leaflet so that phosphatidylserine can be detected *via* annexin V binding.

In our study we have demonstrated that AAF-cmk decreased U937 cell viability what can be qualified as cytotoxic/cytostatic effect *in vitro*. Moreover, the obtained viability reduction was correlated with the number of apoptotic cells detected by annexin V binding. AAF-cmk induced apoptosis *via* the intrinsic

pathway by activation of caspase 9 after 24 h of incubation. We did not observe significant caspase 9 activation upon TNF action, which is known to act along the extrinsic pathway. At this time point, AAF-cmk caused only slight caspase 3 activation in comparison to TNF. After 48 hours the TPPII inhibitor induced apoptosis with the activation of the executor caspase 3, with no further signaling observed for caspase 9. Execution of apoptosis upon AAF-cmk is delayed in comparison to TNF, however, caspase 3 activation obtained with higher inhibitor concentration is comparable to that of TNF.

The discussed above biochemical changes in U937 cells were followed by parallel ultrastructural changes. At the ultrastructural level, apoptosis is characterized by several morphological changes within the nucleus. The chromatin becomes pyknotic and condensed into half-moon shape clumps enclosed within the nuclear envelope. The nucleus undergoes karyorrhexis (fragmentation) by two possible mechanisms, *i.e.* budding and cleavage [34, 35]. The process of nuclear changes during apoptosis, can be divided into four stages [36]. The first ultrastructural hallmark of apoptosis is occurrence of crescent-shaped spaces (CSS) around the nuclear envelope [36].

In U937 treated with AAF-cmk, the first ultrastructural stage of apoptosis is detectable after 24 hours of inhibitor administration. This observation coincides with initiatory caspase activation observed at the same time point. Hence, after 48 hours of inhibitor action, most of cells correspond to ultrastructural stage II (at lower AAF-cmk concentration) or stage III (higher concentration of inhibitor) of apoptosis. In the group with maximal caspase 3 activation (AAF-cmk 40 μM, 48 h), ultrastructural changes are most pronounced. These cells present ultrastructural stage III/IV of apoptosis with karyorrhexis as a sign of apoptotic body formation (stage IV). The observed dominating nucleus fragmentation takes place by the budding mechanism.

Moreover, TEM examination revealed that U937 cells responded to AAF-cmk with autophagy induction and aggregation of proteins. The formation of protein aggregates under proteasome inhibition was first reported by Wojcik *et al.* in 1996 [37–39] and was termed as aggresomes' formation [40]. Aggresomes are localized in the perinuclear ER-rich region, in the proteolytic center of the cell, and form one large structure containing proteasomes and undigested proteins. However, such multifocal type of proteins' aggregates may also be observed in cells upon IFN-γ stimulation that leads to increased protein synthesis. This increased amount of newly synthesized proteins exceeds degradation capability of standard proteasomes resulting in protein aggregation [41]. These multifocal structures are termed aggresome-like structures — ALIS and were first described as DALIS in dendritic cells during their maturation [42, 43]. All these structures accumulate mainly newly synthesized proteins from Defective ribosomal Products (DRiPs) fraction with T1/2 of ca. 10 minutes [42, 43]. The DRiP can constitute up to 30% of newly synthesized proteins and are degraded by UPS [44].

Both aggresomes and ALIS have been shown to be substrates for autophagy [37, 43, 45, 46]. However, autophagy is not the general mechanism for clearance of such protein aggregates [47]. Previous investigations demonstrated that TPPII inhibition decreases activity of pERK1/2, which belong to the MAP kinases family [31]. Activation of the MAP kinase signaling pathway is one of the most potent prosurvival signals in cancer cells. MAP activates downstream mTOR and its inhibition was shown to be one of the key regulators of autophagy [48]. Moreover, cross-talk between autophagy and apoptosis with several proteins has been demonstrated in these two processes [49, 50]. Additionally, autophagy induction can result in cell death and this process is referred as autophagic cell death [51, 52]. In our study, the ultrastructural features of both autophagic and apoptotic cell death, accompanied by secondary necrotic changes, were observed in the same cells.

As TPPII acts primarily downstream to the proteasome, its inhibition can slow proteasome-dependent proteolysis by a feedback loop mechanism, resulting in protein aggregation. In addition, AAF-cmk is known to slightly inhibit chymotrypsin-like activity of the proteasome without affecting its other activities [6]. However, inhibition of only one activity is not sufficient to completely prevent degradation of DRiPs [53]. Moreover, in U937 cells AAF-cmk was shown to induce G0/G1 cell cycle arrest hence proteasome inhibitor (PSI) G2 arrest [6]. Thus the effect of AAF-cmk on U937 probably does not depend on marginal inhibition of chymotripsin-like proteasome activity by this agent.

In our *in vitro* model we observed two types of protein aggregates. The first type was surrounded by ER elements, corresponding to aggresomes or ALIS in the perinuclear region. Furthermore, these aggregates were surrounded by many lysosomal structures, thereby suggesting their involvement in autophagy induction. The second type of aggregates was not related to ER elements, but rather to free cytosolic ribosomes. This type did not correspond to the aggresome neither in localization, nor in the structure, and we refer to these aggregates as ALiSNER (Aggresome-Like Structure Not Associated With the

ER). Their presence can be interpreted as a possible sign of impaired co-translational degradation of proteins on free ribosomes. During protein synthesis, the free N-terminus protrudes from the free ribosome, and as TPPII is an N-terminal peptidase, we suggest that TPPII can be potentially directly involved in trimming of such nascent proteins. In contrast to the proteasome, little is known about the involvement of TPPII in the degradation of nascent proteins, however, TPPII has been recently shown to be localized in close proximity to proteasome [54]. Moreover, we have recently shown in colon adenocarcinoma C26 cells that TPPII is recruited into aggresomes upon proteasome inhibition [55].

As discussed above, TPPII has been linked with proliferation and survival of lymphoma cells and some nonlymphoid tumor cells. These studies were conducted with either TPPII inhibitors, TPPII-specific siRNA, or overexpression of TPPII. However, AAF-cmk itself has been never systematically examined in the context of tumor cell growth and apoptosis induction mechanism. Except our research there are published only few data on the AAF-cmk effect on tumor cell viability. All published data are displayed as controls for the biochemical experiments with both TPPII or/and proteasome inhibitors. In this context AAF-cmk was examined in leukemia cells EL4 and Burkitt lymphoma cells. In EL4 leukemia cells (mouse lymphoblast lymphoma) adapted to the proteasome inhibitor, AAF-cmk in the concentration of 20 μM reduced the cell viability by 80% after 24h incubation [56]. In Burkitt lymphoma cells 10 μM AAF-cmk inhibited growth by 50% after 48h of incubation. Hence 100 μM AAF-cmk completely inhibited the cell growth [30]. However, AAF-cmk at this concentration (100 μM) is not TPPII specific [6].

Thus, the concentration of AAF-cmk applied by other researchers on tumor cells is comparable with the concentrations used by us. Also the average effect of AAF-cmk on cell growth is similar to our results. Moreover we provide novel ultrastructural data on protein aggregation in U937 cells induced by AAF-cmk.

In summary, AAF-cmk reduces viability of leukemic U937 cells and its action results in the formation of two types of cytoplasmic aggregates, triggering of intrinsic apoptosis and autophagy. Further translational study would evaluate application potential of this TPPII inhibitor and detailed mechanism of its cytotoxic activity.

Acknowledgments

We thank Mr. Maciej Krzywicki for excellent graphical assistance. The experimental part of this work was financed by resources of Medical University of Warsaw to LB and IMB (1M15/WB2/08/10) and by the European Regional Development Fund POIG 01.01.02-00-008/08 to GW. The manuscript-handling fee was financed by the Dean of the First Medical Faculty of Medical University of Warsaw, Poland.

Conflict of interest

The authors declare no conflict of interest.

References

1. Rockel B, Peters J, Müller SA, et al. Molecular architecture and assembly mechanism of Drosophila tripeptidyl peptidase II. Proc Natl Acad Sci U S A. 2005; 102(29): 10135–10140, doi: 10.1073/pnas.0504569102, indexed in Pubmed: 16006508.
2. Mlynarczuk-Bialy I. Enigmatic tripeptidylpeptidase II — protease for special tasks. Postepy Biologii Komorki (Advances in Cell Biology). 2008; 35: 427–439.
3. Tomkinson B. Tripeptidyl peptidases: enzymes that count. Trends Biochem Sci. 1999; 24(9): 355–359, indexed in Pubmed: 10470035.
4. Rockel B, Peters J, Kühlmorgen B, et al. A giant protease with a twist: the TPP II complex from Drosophila studied by electron microscopy. EMBO J. 2002; 21(22): 5979–5984, indexed in Pubmed: 12426370.
5. Geier E, Pfeifer G, Wilm M, et al. A giant protease with potential to substitute for some functions of the proteasome. Science. 1999; 283(5404): 978–981, indexed in Pubmed: 9974389.
6. Bury M, Młynarczuk I, Pleban E, et al. Effects of an inhibitor of tripeptidyl peptidase II (Ala-Ala-Phe-chloromethylketone) and its combination with an inhibitor of the chymotrypsin-like activity of the proteasome (PSI) on apoptosis, cell cycle and proteasome activity in U937 cells. Folia Histochem Cytobiol. 2001; 39(2): 131–132, indexed in Pubmed: 11374791.
7. Firat E, Huai J, Saveanu L, et al. Analysis of direct and cross-presentation of antigens in TPPII knockout mice. J Immunol. 2007; 179(12): 8137–8145, indexed in Pubmed: 18056356.
8. Naujokat C, Fuchs D, Berges C. Adaptive modification and flexibility of the proteasome system in response to proteasome inhibition. Biochim Biophys Acta. 2007; 1773(9): 1389–1397, doi: 10.1016/j.bbamcr.2007.05.007, indexed in Pubmed: 17582523.
9. Glas R, Bogyo M, McMaster JS, et al. A proteolytic system that compensates for loss of proteasome function. Nature. 1998; 392(6676): 618–622, doi: 10.1038/33443, indexed in Pubmed: 9560160.
10. Wang EW, Kessler BM, Borodovsky A, et al. Integration of the ubiquitin-proteasome pathway with a cytosolic oligopeptidase activity. Proc Natl Acad Sci U S A. 2000; 97(18): 9990–9995, doi: 10.1073/pnas.180328897, indexed in Pubmed: 10954757.
11. Stavropoulou V, Xie J, Henriksson M, et al. Mitotic infidelity and centrosome duplication errors in cells overexpressing tripeptidyl-peptidase II. Cancer Res. 2005; 65(4): 1361–1368, doi: 10.1158/0008-5472.CAN-04-2085, indexed in Pubmed: 15735022.
12. Stavropoulou V, Vasquez V, Cereser B, et al. TPPII promotes genetic instability by allowing the escape from apoptosis of cells with activated mitotic checkpoints. Biochem Biophys Res Commun. 2006; 346(2): 415–425, doi: 10.1016/j.bbrc.2006.05.141, indexed in Pubmed: 16762321.

13. Sompallae R, Stavropoulou V, Houde M, et al. The MAPK signaling cascade is a central hub in the regulation of cell cycle, apoptosis and cytoskeleton remodeling by tripeptidyl-peptidase II. Gene Regul Syst Bio. 2008; 2: 253–265, indexed in Pubmed: 19787088.
14. Gavioli R, Frisan T, Vertuani S, et al. c-myc overexpression activates alternative pathways for intracellular proteolysis in lymphoma cells. Nat Cell Biol. 2001; 3(3): 283–288, doi: 10.1038/35060076, indexed in Pubmed: 11231578.
15. Duensing S, Darr S, Cuevas R, et al. Tripeptidyl Peptidase II Is Required for c-MYC-Induced Centriole Overduplication and a Novel Therapeutic Target in c-MYC-Associated Neoplasms. Genes Cancer. 2010; 1(9): 883–892, doi: 10.1177/1947601910389605, indexed in Pubmed: 21647238.
16. Hong Xu, Lei Lu, Glas R. Tumors acquire inhibitor of apoptosis protein (IAP)-mediated apoptosis resistance through altered specificity of cytosolic proteolysis. J Exp Med. 2003; 197(12): 1731–1743, doi: 10.1084/jem.20020801, indexed in Pubmed: 12810691.
17. Preta G, de Klark R, Glas R. A role for nuclear translocation of tripeptidyl-peptidase II in reactive oxygen species-dependent DNA damage responses. Biochem Biophys Res Commun. 2009; 389(4): 575–579, doi: 10.1016/j.bbrc.2009.09.021, indexed in Pubmed: 19747897.
18. Młnarczuk I, Mróz P, Hoser G, et al. AAF-cmk sensitizes tumor cells to trail-mediated apoptosis. Leuk Res. 2004; 28(1): 53–61, indexed in Pubmed: 14630081.
19. Hilbi H, Jozsa E, Tomkinson B. Identification of the catalytic triad in tripeptidyl-peptidase II through site-directed mutagenesis. Biochim Biophys Acta. 2002; 1601(2): 149–154, indexed in Pubmed: 12445476.
20. Lévy F, Burri L, Morel S, et al. The final N-terminal trimming of a subaminoterminal proline-containing HLA class I-restricted antigenic peptide in the cytosol is mediated by two peptidases. J Immunol. 2002; 169(8): 4161–4171, indexed in Pubmed: 12370345.
21. Stoltze L, Schirle M, Schwarz G, et al. Two new proteases in the MHC class I processing pathway. Nat Immunol. 2000; 1(5): 413–418, doi: 10.1038/80852, indexed in Pubmed: 11062501.
22. Feleszko W, Jakóbisiak M. Lovastatin augments apoptosis induced by chemotherapeutic agents in colon cancer cells. Clin Cancer Res. 2000; 6(3): 1198–1199, indexed in Pubmed: 10741752.
23. Młynarczuk-Biały I, Roeckmann H, Kuckelkorn U, et al. Combined effect of proteasome and calpain inhibition on cisplatin-resistant human melanoma cells. Cancer Res. 2006; 66(15): 7598–7605, doi: 10.1158/0008-5472.CAN-05-2614, indexed in Pubmed: 16885359.
24. Wójcik C. Proteasomes in apoptosis: villains or guardians? Cell Mol Life Sci. 1999; 56(11-12): 908–917, doi: 10.1007/s000180050483, indexed in Pubmed: 11212325.
25. Hilbi H, Puro RJ, Zychlinsky A. Tripeptidyl peptidase II promotes maturation of caspase-1 in Shigella flexneri-induced macrophage apoptosis. Infect Immun. 2000; 68(10): 5502–5508, indexed in Pubmed: 10992446.
26. Breslin HJ, Miskowski TA, Kukla MJ, et al. Design, synthesis, and tripeptidyl peptidase II inhibitory activity of a novel series of (S)-2,3-dihydro-2-(4-alkyl-1H-imidazol-2-yl)-1H-indoles. J Med Chem. 2002; 45(24): 5303–5310, indexed in Pubmed: 12431057.
27. Ganellin CR, Bishop PB, Bambal RB, et al. Inhibitors of tripeptidyl peptidase II. 2. Generation of the first novel lead inhibitor of cholecystokinin-8-inactivating peptidase: a strategy for the design of peptidase inhibitors. J Med Chem. 2000; 43(4): 664–674, indexed in Pubmed: 10691692.
28. Ganellin CR, Bishop PB, Bambal RB, et al. Inhibitors of tripeptidyl peptidase II. 3. Derivation of butabindide by successive structure optimizations leading to a potential general approach to designing exopeptidase inhibitors. J Med Chem. 2005; 48(23): 7333–7342, doi: 10.1021/jm0500830, indexed in Pubmed: 16279793.
29. Reits E, Neijssen J, Herberts C, et al. A major role for TPPII in trimming proteasomal degradation products for MHC class I antigen presentation. Immunity. 2004; 20(4): 495–506, indexed in Pubmed: 15084277.
30. Villasevil EM, Guil S, López-Ferreras L, et al. Accumulation of polyubiquitylated proteins in response to Ala-Ala-Phe-chloromethylketone is independent of the inhibition of Tripeptidyl peptidase II. Biochim Biophys Acta. 2010; 1803(9): 1094–1105, doi: 10.1016/j.bbamcr.2010.06.001, indexed in Pubmed: 20553980.
31. Wiemhoefer A, Stargardt A, van der Linden WA, et al. Tripeptidyl Peptidase II Mediates Levels of Nuclear Phosphorylated ERK1 and ERK2. Mol Cell Proteomics. 2015; 14(8): 2177–2193, doi: 10.1074/mcp.M114.043331, indexed in Pubmed: 26041847.
32. Pleban E, Bury M, Młynarczuk I, et al. Effects of proteasome inhibitor PSI on neoplastic and non-transformed cell lines. Folia Histochem Cytobiol. 2001; 39(2): 133–134, indexed in Pubmed: 11374792.
33. Makin G, Hickman JA. Apoptosis and cancer chemotherapy. Cell Tissue Res. 2000; 301(1): 143–152, indexed in Pubmed: 10928287.
34. Dini L, Coppola S, Ruzittu MT, et al. Multiple pathways for apoptotic nuclear fragmentation. Exp Cell Res. 1996; 223(2): 340–347, doi: 10.1006/excr.1996.0089, indexed in Pubmed: 8601411.
35. Bonanno E, Ruzittu M, Carlà EC, et al. Cell shape and organelle modification in apoptotic U937 cells. Eur J Histochem. 2000; 44(3): 237–246, indexed in Pubmed: 11095095.
36. Ihara T, Yamamoto T, Sugamata M, et al. The process of ultrastructural changes from nuclei to apoptotic body. Virchows Arch. 1998; 433(5): 443–447, indexed in Pubmed: 9849859.
37. Wójcik C, Schroeter D, Wilk S, et al. Ubiquitin-mediated proteolysis centers in HeLa cells: indication from studies of an inhibitor of the chymotrypsin-like activity of the proteasome. Eur J Cell Biol. 1996; 71(3): 311–318, indexed in Pubmed: 8929570.
38. Wójcik C. On the spatial organization of ubiquitin-dependent proteolysis in HeLa cells. Folia Histochem Cytobiol. 1997; 35(2): 117–118, indexed in Pubmed: 9151102.
39. Wójcik C. An inhibitor of the chymotrypsin-like activity of the proteasome (PSI) induces similar morphological changes in various cell lines. Folia Histochem Cytobiol. 1997; 35(4): 211–214, indexed in Pubmed: 9619420.
40. Johnston JA, Ward CL, Kopito RR. Aggresomes: a cellular response to misfolded proteins. J Cell Biol. 1998; 143(7): 1883–1898, indexed in Pubmed: 9864362.
41. Seifert U, Bialy LP, Ebstein F, et al. Immunoproteasomes preserve protein homeostasis upon interferon-induced oxidative stress. Cell. 2010; 142(4): 613–624, doi: 10.1016/j.cell.2010.07.036, indexed in Pubmed: 20723761.
42. Lelouard H, Gatti E, Cappello F, et al. Transient aggregation of ubiquitinated proteins during dendritic cell maturation. Nature. 2002; 417(6885): 177–182, doi: 10.1038/417177a, indexed in Pubmed: 12000969.
43. Szeto J, Kaniuk NA, Canadien V, et al. ALIS are stress-induced protein storage compartments for substrates of the proteasome and autophagy. Autophagy. 2006; 2(3): 189–199, indexed in Pubmed: 16874109.

44. Schubert U, Antón LC, Gibbs J, et al. Rapid degradation of a large fraction of newly synthesized proteins by proteasomes. Nature. 2000; 404(6779): 770–774, doi: 10.1038/35008096, indexed in Pubmed: 10783891.
45. Dikic I. Proteasomal and Autophagic Degradation Systems. Annu Rev Biochem. 2017; 86: 193–224, doi: 10.1146/annurev-biochem-061516-044908, indexed in Pubmed: 28460188.
46. Wong E, Cuervo AM. Integration of clearance mechanisms: the proteasome and autophagy. Cold Spring Harb Perspect Biol. 2010; 2(12): a006734, doi: 10.1101/cshperspect.a006734, indexed in Pubmed: 21068151.
47. Wong ESP, Tan JMM, Soong WE, et al. Autophagy-mediated clearance of aggresomes is not a universal phenomenon. Hum Mol Genet. 2008; 17(16): 2570–2582, doi: 10.1093/hmg/ddn157, indexed in Pubmed: 18502787.
48. Jung CH, Ro SH, Cao J, et al. mTOR regulation of autophagy. FEBS Lett. 2010; 584(7): 1287–1295, doi: 10.1016/j.febslet.2010.01.017, indexed in Pubmed: 20083114.
49. Wojcik S. Crosstalk between autophagy and proteasome protein degradation systems: possible implications for cancer therapy. Folia Histochem Cytobiol. 2013; 51(4): 249–264, doi: 10.5603/FHC.2013.0036, indexed in Pubmed: 24497130.
50. Li M, Gao P, Zhang J. Crosstalk between Autophagy and Apoptosis: Potential and Emerging Therapeutic Targets for Cardiac Diseases. Int J Mol Sci. 2016; 17(3): 332, doi: 10.3390/ijms17030332, indexed in Pubmed: 26950124.
51. Maiuri MC, Zalckvar E, Kimchi A, et al. Self-eating and self-killing: crosstalk between autophagy and apoptosis. Nat Rev Mol Cell Biol. 2007; 8(9): 741–752, doi: 10.1038/nrm2239, indexed in Pubmed: 17717517.
52. Levine B, Yuan J. Autophagy in cell death: an innocent convict? J Clin Invest. 2005; 115(10): 2679–2688, doi: 10.1172/JCI26390, indexed in Pubmed: 16200202.
53. Kisselev AF, Callard A, Goldberg AL. Importance of the different proteolytic sites of the proteasome and the efficacy of inhibitors varies with the protein substrate. J Biol Chem. 2006; 281(13): 8582–8590, doi: 10.1074/jbc.M509043200, indexed in Pubmed: 16455650.
54. Fukuda Y, Beck F, Plitzko JM, et al. In situ structural studies of tripeptidyl peptidase II (TPPII) reveal spatial association with proteasomes. Proc Natl Acad Sci U S A. 2017; 114(17): 4412–4417, doi: 10.1073/pnas.1701367114, indexed in Pubmed: 28396430.
55. Bialy LP, Kuckelkorn U, Henklein P, et al. Changes in spatio-temporal localization of tripeptidyl peptidase II (TPPII) in murine colon adenocarcinoma cells during aggresome formation: a microscopy study based on a novel fluorescent proteasome inhibitor. Histol Histopathol. 2018, doi: 10.14670/HH-18-042, indexed in Pubmed: 30226264.
56. Princiotta MF, Schubert U, Chen W, et al. Cells adapted to the proteasome inhibitor 4-hydroxy- 5-iodo-3-nitrophenylacetyl-Leu-Leu-leucinal-vinyl sulfone require enzymatically active proteasomes for continued survival. Proc Natl Acad Sci U S A. 2001; 98(2): 513–518, doi: 10.1073/pnas.021132398, indexed in Pubmed: 11149939.

Submitted: 12 February, 2018
Accepted after reviews: 30 September, 2018
Available as AoP: 5 October, 2018